Title

Metabolomic changes in murine serum following inhalation exposure to gasoline and diesel engine emissions

Journal

Inhalation Toxicology, 28(5)

ISSN

0895-8378

Authors

Brower, Jeremy B
Doyle-Eisele, Melanie
Moeller, Benjamin
et al.

Publication Date

2016-04-15

DOI

10.3109/08958378.2016.1155003

Peer reviewed

HHS Public Access

Author manuscript

Inhal Toxicol. Author manuscript; available in PMC 2017 April 01.

Published in final edited form as:

Inhal Toxicol. 2016 April ; 28(5): 241–250. doi:10.3109/08958378.2016.1155003.

Metabolomic Changes in Murine Serum Following Inhalation Exposure to Gasoline and Diesel Engine Emissions

Jeremy B. Brower[1], **Melanie Doyle-Eisele**[1], **Benjamin Moeller**[1], **Steven Stirdivant**[2], **Jacob D. McDonald**[1], and **Matthew J. Campen**[3]

[1]Lovelace Respiratory Research Institute, Albuquerque, NM

[2]Metabolon, Inc., Durham, NC

[3]College of Pharmacy, University of New Mexico, Albuquerque, NM, 87131

Abstract

The adverse health effects of environmental exposure to gaseous and particulate components of vehicular emissions are a major concern among urban populations. A link has been established between respiratory exposure to vehicular emissions and the development of cardiovascular disease (CVD), but the mechanisms driving this interaction remain unknown. Chronic inhalation exposure to mixed vehicle emissions has been linked to CVD in animal models. This study evaluated the temporal effects of acute exposure to mixed vehicle emissions (MVE; mixed gasoline and diesel emissions) on potentially active metabolites in the serum of exposed mice. C57Bl/6 mice were exposed to a single 6 hour exposure to filtered air (FA) or MVE (100 or 300 μg/m^3) by whole body inhalation. Immediately after and 18 hours after the end of the exposure period, animals were sacrificed for serum and tissue collection. Serum was analyzed for metabolites that were differentially present between treatment groups and time points. Changes in metabolite levels suggestive of increased oxidative stress (oxidized glutathione, cysteine disulfide, taurine), lipid peroxidation (13-HODE, 9-HODE), energy metabolism (lactate, glycerate, branched chain amino acid catabolites, butrylcarnitine, fatty acids), and inflammation (DiHOME, palmitoyl ethanolamide) were observed immediately after the end of exposure in the serum of animals exposed to MVE relative to those exposed to FA. By 18 hours post exposure, serum metabolite differences between animals exposed to MVE versus those exposed to FA were less pronounced. These findings highlight complex metabolomics alterations in the circulation following inhalation exposure to a common source of combustion emissions.

Keywords

cardiovascular; diesel; particulate matter; air pollution; metabolomics; oxidized lipids

Corresponding Author: Matthew J. Campen, MSC09 5360, 1 University of New Mexico, Albuquerque, NM 87131, 505 925-7778, mcampen@salud.unm.edu.

INTRODUCTION

Air pollution has a well-established cardiovascular health impact (Brook et al., 2010; Langrish et al., 2012; Pope et al., 1999). The World Health Organization estimates that annually 7 million people die prematurely globally as a result of air pollution exposure, and most of these deaths appear due to cardiovascular sequelae (Brook et al., 2010; Samet and Krewski, 2007). What remains unclear is how inhaled pollutants, most of which are not absorbed well systemically, are able to cause adverse pathology at sites beyond the lung. Toxicological studies clearly demonstrate health effects arising in extrapulmonary compartments, such as the heart, aorta, brain, and adipose tissue (Block and Calderon-Garciduenas, 2009; Calderon-Garciduenas et al., 2012; Kampfrath et al., 2011; Levesque et al., 2011; Lund et al., 2011; Lund et al., 2009; Lundback et al., 2009; Sun et al., 2005). While particulate matter (PM) and other gaseous pollutants can be taken up and access extrapulmonary sites, the net transfer is quite low and it has yet to be established that a direct effect is responsible for pathological findings.

Our recent studies have explored the potential for indirect effects of inhaled pollutants to be carried in the circulation, focusing on assessments of bioactivity in serum from exposed humans and animals. Diesel exhaust inhalation induced a pro-inflammatory activity in serum of healthy human subjects, in that the serum more potently elevated transcription of adhesion molecules and cytokines in cultured endothelial cells (Channell et al., 2012; Schisler et al., 2015b). More recently, we have noted that inhalation of ozone, which reacts completely in the lung and does not pass beyond the surfactant layer intact, led to changes in the serum that diminished endothelial-dependent vasodilation in rats and mice, and the scavenger receptor CD36 appears to have a prominent intermediary role (Paffett et al., 2015; Robertson et al., 2013). Similarly, nickel nanoparticle inhalation exposures drive a serum bioactivity that impairs angiogenesis in vitro (Liberda et al., 2014). The consistency among inhalation studies of various PM and various gases in terms of this inflammatory serum potential strongly argues for the generation of bioactive intermediary circulating factors.

While cytokines such as IL-6 or TGF-beta are plausible candidates for mediating vascular or neuroinflammation, both human and rodent studies infrequently find these and similar cytokines to be elevated (Mills et al., 2005; Schisler et al., 2015b). We therefore collected murine serum samples following exposure conditions known to induce bioactivity and assessed changes in small molecule metabolites in a high-throughput manner to test whether substantial changes in this category of serum components might inform the pathogenesis of extrapulmonary outcomes.

METHODS

Animals

Male, 8–10 week old C57BL/6 mice were obtained from a commercial vendor (Taconic) and placed in quarantine 2 weeks prior to exposure. Mice were single-housed in AAALAC-approved conditions for light cycle (12 hour light-dark cycle), temperature and humidity on Sani-Chips bedding. Monitoring of environmental conditions for the period of quarantine and exposure showed a range of temperatures from 21.9 – 24.7°C and relative humidity

from 42 – 56 %. Food and water were available ad libitum, expect during exposures when food was removed from cages. Animals were weighed for randomization prior to the start of exposures. Following exposures, mice were euthanized by humane means (barbiturate overdose). All studies were approved by the Lovelace Respiratory Research Institute's Animal Care and Use Committee.

Generation of MVE Exposure Atmospheres

Similar to previous studies, (Lund et al., 2011; Vedal et al., 2013) MVE was composed of a mixture of freshly generated gasoline and diesel engine exhausts. Target PM concentrations of 100 and 300 μg/m^3 were implemented, with roughly 80% of PM mass coming from the diesel engine and 20% from the gasoline engine. The diesel generator (Yanmar) was run on a constant (high) operating load, while the gasoline engine was operated on a specific driving cycle using a dynamometer, as previously described (Vedal et al., 2013). The exhausts were combined in a mixing chamber upstream of the exposure chamber and diluted with filtered air to achieve the final target concentrations.

Exposure Study Design

Mice (N=6 per group; 36 total) were subjected to a single, continuous 6-h exposure of filtered air (FA), 100 μg/m^3 or 300 μg/m^3 of MVE, beginning at approximately 6:30 am, 30 minutes after lights had turned on for the day. Mice were euthanized either immediately following (0 hour time point (approximately 12:30 pm) or 18 h following exposure (approximately 6:30 am the following day). Serum was collected and flash frozen for metabolomics analysis.

Exposure System

Mice were exposed individually housed in shoebox microisolator cages with the filter lids removed and dust-free techboard (Untreated technical-grade deotized animal cage board) replacing standard bedding chips, placed inside of Hazelton H1000 whole body inhalation exposure chambers (Lab Products, Seaford, DE). Total airflow through the exposure chambers was maintained at 150–200 L/min.

Sample Accessioning

Each sample received was accessioned into the Metabolon LIMS system and was assigned by the LIMS a unique identifier, which was associated with the original source identifier only. This identifier was used to track all sample handling, tasks, results, *etc.* The samples (and all derived aliquots) were bar-coded and tracked by the LIMS system. All portions of any sample were automatically assigned their own unique identifiers by the LIMS when a new task was created; the relationship of these samples was also tracked. All samples were maintained at −80 °C until processed.

Sample Preparation

The sample preparation process was carried out using the automated MicroLab STAR® system from Hamilton Company. Recovery standards were added prior to the first step in the extraction process for QC purposes. Sample preparation was conducted using a proprietary

series of organic and aqueous extractions to remove the protein fraction while allowing maximum recovery of small molecules. The resulting extract was divided into two fractions; one for analysis by UPLC-MS/MS and one for analysis by GC/MS. Samples were placed briefly on a TurboVap® (Zymark) to remove the organic solvent. Each sample was then frozen and dried under vacuum. Samples were then prepared for the appropriate instrument, either LC/MS or GC/MS.

QA/QC

For QA/QC purposes, a number of additional samples were included with each day's analysis. Furthermore, a selection of QC compounds was added to every sample, including those under test. These compounds were carefully chosen so as not to interfere with the measurement of the endogenous compounds. These QC samples were primarily used to evaluate the process control for each study as well as aiding in the data curation.

Liquid chromatography/Mass Spectrometry (LC/MS, LC/MS^2)

The LC/MS portion of the platform was based on a Waters ACQUITY UPLC and a Thermo-Finnigan LTQ mass spectrometer, which consisted of an electrospray ionization (ESI) source and linear ion-trap (LIT) mass analyzer. The sample extract was split into two aliquots, dried, then reconstituted in acidic or basic LC-compatible solvents, each of which contained 11 or more injection standards at fixed concentrations. One aliquot was analyzed using acidic positive ion optimized conditions and the other using basic negative ion optimized conditions in two independent injections using separate dedicated columns. Extracts reconstituted in acidic conditions were gradient eluted using water and methanol both containing 0.1% Formic acid, while the basic extracts, which also used water/methanol, contained 6.5mM Ammonium Bicarbonate. The MS analysis alternated between MS and data-dependent MS^2 scans using dynamic exclusion.

Gas chromatography/Mass Spectrometry (GC/MS)

The samples destined for GC/MS analysis were re-dried under vacuum desiccation for a minimum of 24 hours prior to being derivatized under dried nitrogen using bistrimethyl-silyl-triflouroacetamide (BSTFA). The GC column was 5% phenyl and the temperature ramp was from 40° to 300° C in a 16 minute period. Samples were analyzed on a Thermo-Finnigan Trace DSQ fast-scanning single-quadrupole mass spectrometer using electron impact ionization. The instrument was tuned and calibrated for mass resolution and mass accuracy on a daily basis. The information output from the raw data files was automatically extracted as discussed below.

Bioinformatics

The informatics system consisted of four major components, the Laboratory Information Management System (LIMS), the data extraction and peak-identification software, data processing tools for QC and compound identification, and a collection of information interpretation and visualization tools for use by data analysts. The hardware and software foundations for these informatics components were the LAN backbone, and a database server running Oracle 10.2.0.1 Enterprise Edition.

Data Extraction and Compound Identification

Raw data was extracted, peak-identified and QC processed using Metabolon's hardware and software. Compounds were identified by comparison to library entries of purified standards or recurrent unknown entities. Metabolon maintains a library based on authenticated standards that contains the retention time/index (RI), mass to charge ratio (*m/z*), and chromatographic data (including MS/MS spectral data) on all molecules present in the library. Furthermore, biochemical identifications are based on three criteria: retention index within a narrow RI window of the proposed identification, nominal mass match to the library +/− 0.4 amu, and the MS/MS forward and reverse scores between the experimental data and authentic standards. The MS/MS scores are based on a comparison of the ions present in the experimental spectrum to the ions present in the library spectrum. While there may be similarities between these molecules based on one of these factors, the use of all three data points can be utilized to distinguish and differentiate biochemicals. More than 3500 commercially available purified standard compounds have been acquired and registered into LIMS for distribution to both the LC-MS and GC-MS platforms for determination of their analytical characteristics.

Curation

A variety of curation procedures were carried out to ensure that a high quality data set was made available for statistical analysis and data interpretation. The QC and curation processes were designed to ensure accurate and consistent identification of true chemical entities, and to remove those representing system artifacts, mis-assignments, and background noise. Metabolon data analysts use proprietary visualization and interpretation software to confirm the consistency of peak identification among the various samples. Library matches for each compound were checked for each sample and corrected if necessary.

Statistical Calculation

Data were compared by a two-way ANOVA, treating time and exposure concentration as experimental factors, with Bonferroni post-hoc testing to compare exposure effects against control. Six samples per group were available for data analysis. Probability values less than 0.05 were considered significant, but further consideration was given to trends observed in the range of 0.05–0.10.

RESULTS

Animals

Mice were weighed prior to the start of exposures for purposes of randomizing into exposure groups. Animals with the lowest and highest body weights were excluded as spares. The body weights of those animals used on study ranged from 23.9 – 31.8 g. After exposures, the animals appeared healthy and demonstrated no overt signs of toxicity. Terminal body weights were not appreciably different from pre-exposure body weights.

Exposures

Target conditions for the single day exposure, based on particulate matter mass concentrations, were 0, 100, and 300 μg/m^3. Actual measurements, representing the average of 3 samples obtained throughout the 6 h exposure, were within 15% of target, at 0, 113, and 390 μg/m^3 (Table 1). Associated gases NOx and CO were measured, as well, and were not as proportionately distributed as PM (Table 1), but consistent with previous work (Vedal 2013).

Serum Metabolomic Changes: Overview

Serum was analyzed using the multiple mass spec platforms and 382 known biomolecules were measured in the samples. The study design incorporated both exposure concentration and time (0h and 18h post exposure) as independent factors. Metabolite changes were therefore assessed across both time and concentration. Time potentially reflects contributions from circadian differences, though these changes could also be reflective of random variation. At the $p<0.05$ criteria, we observed a total of 65 biochemicals at higher levels and 12 at lower levels at 18 h post-exposure to filtered air (FA) compared to 0h post-exposure (Table 2). In the MVE100 group, circadian rhythm differences coupled with MVE exposure led to 45 biochemicals at higher levels and 62 biochemical at lower levels, while in the MVE300 group, the circadian differences plus MVE exposure led to 32 biochemicals at higher levels and 29 biochemical at lower levels. The differences in these numbers suggest some perturbation of circadian homeostasis by MVE exposure.

At 0h post exposure, the MVE100 atmosphere induced 109 metabolites at higher levels and 5 at lower levels at the $p<0.05$ level and 135 at higher levels and 12 at lower levels at the $p<0.10$ level, relative to 0 hr FA controls. The MVE300 atmosphere had a lesser impact, leading to increases in 30 biochemicals and lower levels in 1 at $p<0.05$ and increasing 53 and decreasing 3 biochemicals at the $p<0.10$ threshold, relative to 0 hr FA controls. At the 18h timepoint, ANOVA revealed metabolite changes specific for the MVE100 concentration numbered 24 (7 up, 17 down) at the $p<0.05$ criteria and 43 (13 up, 30 down) at the $p<0.10$ criteria vs. 18 hr FA controls (Table 3). Two-way ANOVA interactions between concentration and time revealed significant metabolite changes numbering 18 at the $p<0.05$ criteria and 33 at the $p<0.10$ criteria (Table 4).

Serum Metabolomic Changes: Specific Biochemicals

Notably, biochemicals related to tryptophan metabolism were consistently different between 0h and 18h groups in all exposure concentrations, reflecting the importance and robust nature of this pathway in regulating circadian rhythm (see Supplemental Table 1) (Pietraszek et al., 1992). Other biochemicals were similarly modulated by circadian differences, but unaffected by exposure, including arginine, methionine, urea, several gamma-glutamyl amino acids, 2-aminophenol sulfate and several molecules relevant to benzoate metabolism (Tables 5, 6).

Exposure to MVE led to both concentration–dependent and –independent changes in numerous serum biochemicals. Among the more profoundly altered biochemicals immediately after the MVE exposure was oxidized glutathione (GSSG), which was elevated

2.8 and 1.9-fold in the MVE100 ($p<0.05$) and MVE300 ($p=0.07$) groups, respectively. Similarly, elevated levels of cysteine-glutathione disulfide were observed in both groups, albeit at lower inductions (1.45, $p<0.05$ and 1.3-fold, $p=0.052$, respectively), also an indication of oxidation of this protective thiol. Additional evidence for oxidative stress was noted for circulating levels of 13-HODE+9-HODE and 12,13-DiHOME, both of which were significantly elevated in the MVE100 group (2.8 and 2.4-fold, respectively), but showed only non-significant increasing trends in the MVE300 group immediately following exposure. Other consistently altered biochemicals at the 0h timepoint included 2-ethylhexanoate (1.45 and 1.56-fold induction in MVE100 and MVE300, respectively), 2-pyrrolidinone (1.29 and 1.22-fold induction in MVE100 and MVE300, respectively), and valerylcarnitine (1.82 and 1.53-fold induction in MVE100 and MVE300, respectively).

Few changes in metabolites were noted at the 18h post-exposure timepoint that were consistent in both MVE concentrations. 1-lignoceroylglycerophosphocholine (24:0) notably was substantially reduced, present at only 11% and 7% of control levels in the MVE100 and MVE300 groups, respectively. Several other lysolipids were significantly reduced in the MVE100 group, but typically not in the MVE300 group. Serum levels of 4-hydroxyhippurate and stachydrine were also reduced in both exposure groups at the 18h timepoint.

Several other notable changes occurred that were inconsistent between exposure groups, most frequently occurring in the low MVE concentration exposure. Immediately following exposures, induction of medium [caproate (6:0), caprylate (8:0)] and long-chain [myristate (14:0), myristoleate (14:1n5), oleate (18:1n9)] fatty acids, along with metabolites derived from fatty acid metabolism (butyrylcarnitine, valerylglycine) was noted in the MVE100 group, relative to FA controls.. Adenosine was significantly reduced (14% of control) in the MVE100 group immediately after exposures. At 18h following the MVE100 exposure, potent induction of the bile acids deoxycholate (4.6-fold) and taurodeoxycholate (3.3-fold) were noted. Bradykinin was significantly elevated in the MVE100 exposure group, relative to FA controls, at both timepoints (3.4-fold at 0h and 3.3-fold at 18h). Lastly, a fibrinogen cleavage product, TDTEDKGEFLSEGGGVR showed similar induction at both timepoints in the MVE100 group, relative to FA controls, but was only significantly elevated at 18h (3.0-fold, n.s. at 0h and 2.6-fold, $p<0.05$ at 18h).

In the MVE300 group, several components of amino acid metabolism (2-methylbutyrylglycine, 2-hydroxy-3-methylvalerate, 3-methyl-2-oxobutyrate, alpha-hydroxyisocaproate, taurine, creatine) were significantly elevated immediately after exposure, as were several biochemical involved in energy production (mannose, lactate, glycerate).

DISCUSSION

The present study documents a panel of serum metabolite alterations induced by inhalation exposure to a mixture of gasoline and diesel engine exhausts. Alterations suggest perturbation to a number of metabolic processes, but the nature of this disruption is complicated by the factors of time and concentration. Circadian rhythm caused substantial

changes in serum biochemistry in control mice, and MVE exposures appeared to disrupt these patterns. MVE exposure induced several factors reflective of oxidative stress (oxidized glutathione, 13-HODE, 9-HODE) and altered fatty acid metabolism. In recent human and rodent studies, inhalation exposure to a wide variety of pollutants renders a pro-inflammatory bioactivity in the serum that can cause induction of inflammatory genes in cultured endothelial cells or impair vasodilation in isolated arteries (Aragon et al., 2015; Channell et al., 2012; Robertson et al., 2013; Schisler et al., 2015a). Metabolomic findings in the present study are consistent with serum alterations resulting from inhalation exposures, but it remains unclear if any specific alterations described herein cause this bioactivity.

Inhalation of particles and gases cause systemic pathologies, including inflammation of arteries, adipose, and neural tissues, vasoconstriction and atherosclerotic remodeling (Campen et al., 2014; Sun et al., 2005; Vedal et al., 2013). MVE specifically has been extensively characterized in mouse models and has clear vasculotoxic effects (Aragon et al., 2015; Lund et al., 2011; Vedal et al., 2013). The underlying mechanism for such changes appears to be indirect, as particulates directly applied to vessels or cultured endothelial cells or directly injected intravenously often fail to recapitulate the vascular effects of relevant concentrations of inhaled particulates. Bioactivity of serum obtained after exposure strongly argues for indirect effects of secondary circulating factors arising from the lung. Numerous studies have attempted to measure inflammatory cytokines in the serum following various exposures. While a few studies have reported strong evidence for induction of factors such as IL-6 (Mutlu et al., 2007), MMP-9 (Lund et al., 2009), or ET-1 (Lund et al., 2009; Thomson et al., 2005), other studies fail to reproduce such findings. Conventional cytokines such as CRP and TNFa are frequently reported, but rarely change as a result of environmentally relevant exposures. In numerous human exposure studies with diesel emissions, circulating cytokines are rarely increased (Mills et al., 2007; Mills et al., 2005) and panel and epidemiological studies yield inconsistent but modest alterations to circulating cytokines in relation to ambient PM levels (Bind et al., 2012; Delfino et al., 2008). While mechanistic rodent work has provided compelling evidence for a pathological role for cytokines such as IL6 (Mutlu et al., 2007) and the CCR2/CCL2 axis (Liu et al., 2014), such findings fail to fully explain findings in controlled exposure human studies. Thus, it is logical to pursue high-throughput assessments of serum biochemical changes caused by exposures.

A number of lipid metabolites associated with lipid peroxidation or inflammation were increased in the MVE-exposed groups; although increases were generally greater in the MVE100 group. 13-HODE/9-HODE are measures of lipid peroxidation and they were elevated to a statistically significant level in the MVE100 group relative to FA controls. Elevated 13-HODE/9-HODE is consistent with diesel exposure studies, wherein 13-HODE was 2.5-fold induced in the plasma following a 2-week exposure to 250 $\mu g/m^3$, and this alteration persisted for over a week (Yin et al., 2013). Here, we see that a mix of gasoline and diesel emissions induced a similar effect observable after a single 6h exposure. In addition, oxalate, which has been correlated with lipid peroxidation in some tissues (Huang et al., 2003) was elevated to a statistically significant level in the MVE100 0h group. 12, 13-DiHOME and palmitoyl ethanolamide are two lipid derivatives reported to be modulators of

inflammatory activity. 12, 13-DiHOME has been reported to be a neutrophil attractant and may indicate increased inflammation (HMDB04705). Palmitoyl ethanolamide has anti-inflammatory activity and may accumulate in blood following tissue injury (HMDB02100). In addition, 12-HETE is derived from lipoxygenase activity on arachidonic acid and has been reported to act as a vasoconstrictor (HMDB06111). Overall, the data may suggest that MVE exposure may increase lipid peroxidation and cause modulation of lipid regulated inflammatory mechanisms.

Two markers of oxidative stress, oxidized glutathione and cysteine-glutathione disulfide, were observed to be increased as a result of MVE exposure. Levels of oxidized glutathione and cysteine-glutathione disulfide, in MVE serums, returned to control levels at the 18-hour time point. Taurine, an anti-oxidant, was increased to a statistically significant degree in the MVE300 group relative to FA controls at 0 hours and may reflect a response to increased oxidative stress. Cysteine, which is an intermediate in taurine and glutathione synthesis was also elevated in the MVE100 and MVE300 groups relative to control, but statistical significance was only achieved for the MVE300 group at a $p<0.1$ level. The cluster of increases in the cysteine/glutathione synthesis pathway may represent increased systemic oxidative stress along with a compensatory response to generate more anti-oxidants. By 18 hours the differences between MVE exposed serums and FA controls was negligible.

The levels of a set of metabolites with cardiovascular activity or that are related to cardiovascular active biochemicals were found to change with MVE exposure. The metabolites bradykinin (HMDB04246) and adenosine (HMDB00050) both have vasodilator activity. In addition, adenosine has also been reported to have vasoconstrictor activity in some tissues (Carlstrom et al., 2009) and has an important role in stimulating angiogenesis (Feoktistov et al., 2009). Bradykinin levels were up in both the MVE100 and MVE300 0-hour groups, relative to FA-0 hour controls (though only statistically significant for MVE100). Bradykinin remained elevated at 18 hours in the MVE100 18-hour serums. Adenosine was dramatically reduced in the MVE100 0-hour serums (14% of control; $p=0.0006$) and also lower in MVE300 0-hour serums (66% of control; $p=0.094$). Also of interest was a decrease in histidine with a commensurate rise in 1-methylimidazoleacetate in MVE100 0-hour serums. The vasodilator histamine is produced from histidine, and 1-methylimidazoleacetate is a degradation product of histamine. It is possible that more histidine is being used to produce histamine, with an increase in 1-methylimidazoleacetate resulting from an increased serum histamine level (histamine was below the level of detection in these serums). Arginine, from which nitric oxide (NO) is derived, through the activity of nitric oxide synthase, was decreased in MVE100 0-hour serums relative to FA 0-hour controls and might possibly be an indication of increased NO production. Finally, two fibrinogen peptide fragments were elevated in all MVE exposed serums relative to FA controls, but statistical significance was only achieved in the comparison of MVE300 18-hour serums to FA 18-hour serums. Increases in fibrinogen fragments have been linked to inflammation and injured vessel walls. Increases in fibrinogen fragments might also reflect extracellular matrix remodeling or an impact on the vascular clotting system. It was interesting that changes were greater in the MVE100 than in the MVE300 serums as one might expect an MVE concentration response to generate the opposite finding.

A major limitation of the present study was our inability to clearly link metabolomics changes to any health outcomes known to be related to environmental exposure to pollutants in MVE. Importantly, with dozens of individual components altered by time and exposure, and in complex patterns of change, it would be highly challenging to ascribe health outcomes to any single metabolite. First, a metabolite would have to be able to drive any specific health outcome by itself, and all other metabolites would need to be tested to confirm that they did not induce such changes. The overall degree of induction for metabolites was quite low, often less than 100% above control, which we feel is unlikely to be sufficient to cause pathological alterations. Several factors that were 3-fold induced may merit follow-up studies, including bradykinin and fibrinogen cleavage products, along with 13-HODE+9-HODE and 12,13-DiHOME. However, even establishing the potential for such metabolites to drive pathological outcomes in research models, we have still not addressed biochemical changes to larger molecules/protein (expression, modification) or subcellular components (microvessicles), which would all require separate analytical platforms.

Concentrations of the MVE in the present study are high relative to ambient conditions in the United States, but relate well to air pollution levels in many industrial regions of the world, such as China and India, where likely billions of people are exposed. Most of the metabolomics changes in the present study were seen after a 6h exposure to a 100 $\mu g/m^3$ concentration. Over a 24h period, this averages to only 25 $\mu g/m^3$, which is only twice the current United States National Ambient Air Quality Standard for $PM_{2.5}$. Gaseous components are also present in this combustion mixture, with carbon monoxide being approximately 5 times the 8h standard and NO_X being roughly 70-fold higher than the 1h standard of 100 ppb. However, NO_X levels in the MVE atmosphere are predominantly (>90%) nitric oxide with only a small contribution of the more toxic nitrogen dioxide (Vedal et al., 2013).

In summary, the present metabolomic characterization of serum from mice exposed to short-term vehicular emissions revealed a variety of changes that suggest alterations to fatty acid and amino acid metabolism, energy production, and oxidative markers. The breadth of metabolomic outcomes is consistent with findings of serum-borne inflammatory bioactivity (Aragon et al., 2015), in that numerous metabolites were altered, but the outcomes fail to clearly identify potential intermediate drivers of vascular pathology. More extensive and comprehensive characterization of circulatory alterations following inhalation exposures to particles and gases, along with linkages to functional outcomes, is therefore necessary.

Supplementary Material

Refer to Web version on PubMed Central for supplementary material.

Acknowledgments

Acknowledgements and Funding: This study was funded by grants from the National Institutes of Health (ES014639) and the Environmental Protection Agency (RD-83479601-0). The views expressed in this document are solely those of the authors and the U.S. EPA does not endorse any products or commercial services mentioned in this publication.

References

Aragon MJ, Chrobak I, Brower J, Roldan L, Fredenburgh LE, McDonald JD, Campen MJ. Inflammatory and Vasoactive Effects of Serum Following Inhalation of Varied Complex Mixtures. Cardiovasc Toxicol. 2015

Bind MA, Baccarelli A, Zanobetti A, Tarantini L, Suh H, Vokonas P, Schwartz J. Air pollution and markers of coagulation, inflammation, and endothelial function: associations and epigene-environment interactions in an elderly cohort. Epidemiology. 2012; 23:332–340. [PubMed: 22237295]

Block ML, Calderon-Garciduenas L. Air pollution: mechanisms of neuroinflammation and CNS disease. Trends Neurosci. 2009; 32:506–516. [PubMed: 19716187]

Brook RD, Rajagopalan S, Pope CA 3rd, Brook JR, Bhatnagar A, Diez-Roux AV, Holguin F, Hong Y, Luepker RV, Mittleman MA, Peters A, Siscovick D, Smith SC Jr, Whitsel L, Kaufman JD. American Heart Association Council on, E., Prevention, C.o.t.K.i.C.D., Council on Nutrition, P.A., Metabolism. Particulate matter air pollution and cardiovascular disease: An update to the scientific statement from the American Heart Association. Circulation. 2010; 121:2331–2378. [PubMed: 20458016]

Calderon-Garciduenas L, Kavanaugh M, Block M, D'Angiulli A, Delgado-Chavez R, Torres-Jardon R, Gonzalez-Maciel A, Reynoso-Robles R, Osnaya N, Villarreal-Calderon R, Guo R, Hua Z, Zhu H, Perry G, Diaz P. Neuroinflammation, hyperphosphorylated tau, diffuse amyloid plaques, and down-regulation of the cellular prion protein in air pollution exposed children and young adults. Journal of Alzheimer's disease : JAD. 2012; 28:93–107. [PubMed: 21955814]

Campen M, Robertson S, Lund A, Lucero J, McDonald J. Engine exhaust particulate and gas phase contributions to vascular toxicity. Inhal Toxicol. 2014; 26:353–360. [PubMed: 24730681]

Carlstrom M, Lai EY, Ma Z, Patzak A, Brown RD, Persson AE. Role of NOX2 in the regulation of afferent arteriole responsiveness. Am J Physiol Regul Integr Comp Physiol. 2009; 296:R72–R79. [PubMed: 18987286]

Channell MM, Paffett ML, Devlin RB, Madden MC, Campen MJ. Circulating factors induce coronary endothelial cell activation following exposure to inhaled diesel exhaust and nitrogen dioxide in humans: evidence from a novel translational in vitro model. Toxicol Sci. 2012; 127:179–186. [PubMed: 22331494]

Delfino RJ, Staimer N, Tjoa T, Polidori A, Arhami M, Gillen DL, Kleinman MT, Vaziri ND, Longhurst J, Zaldivar F, Sioutas C. Circulating biomarkers of inflammation, antioxidant activity, and platelet activation are associated with primary combustion aerosols in subjects with coronary artery disease. Environ Health Perspect. 2008; 116:898–906. [PubMed: 18629312]

Feoktistov I, Biaggioni I, Cronstein BN. Adenosine receptors in wound healing, fibrosis and angiogenesis. Handbook of experimental pharmacology. 2009:383–397. [PubMed: 19639289]

Huang HS, Ma MC, Chen CF, Chen J. Lipid peroxidation and its correlations with urinary levels of oxalate, citric acid, and osteopontin in patients with renal calcium oxalate stones. Urology. 2003; 62:1123–1128. [PubMed: 14665375]

Kampfrath T, Maiseyeu A, Ying Z, Shah Z, Deiuliis JA, Xu X, Kherada N, Brook RD, Reddy KM, Padture NP, Parthasarathy S, Chen LC, Moffatt-Bruce S, Sun Q, Morawietz H, Rajagopalan S. Chronic fine particulate matter exposure induces systemic vascular dysfunction via NADPH oxidase and TLR4 pathways. Circ Res. 2011; 108:716–726. [PubMed: 21273555]

Langrish JP, Bosson J, Unosson J, Muala A, Newby DE, Mills NL, Blomberg A, Sandstrom T. Cardiovascular effects of particulate air pollution exposure: time course and underlying mechanisms. J Intern Med. 2012; 272:224–239. [PubMed: 22724512]

Levesque S, Taetzsch T, Lull ME, Kodavanti U, Stadler K, Wagner A, Johnson JA, Duke L, Kodavanti P, Surace MJ, Block ML. Diesel exhaust activates and primes microglia: air pollution, neuroinflammation, and regulation of dopaminergic neurotoxicity. Environmental health perspectives. 2011; 119:1149–1155. [PubMed: 21561831]

Liberda EN, Cuevas AK, Qu Q, Chen LC. The acute exposure effects of inhaled nickel nanoparticles on murine endothelial progenitor cells. Inhal Toxicol. 2014; 26:588–597. [PubMed: 25144474]

Liu C, Xu X, Bai Y, Wang TY, Rao X, Wang A, Sun L, Ying Z, Gushchina L, Maiseyeu A, Morishita M, Sun Q, Harkema JR, Rajagopalan S. Air pollution-mediated susceptibility to inflammation and insulin resistance: influence of CCR2 pathways in mice. Environ Health Perspect. 2014; 122:17–26. [PubMed: 24149114]

Lund AK, Lucero J, Harman M, Madden MC, McDonald JD, Seagrave JC, Campen MJ. The oxidized low-density lipoprotein receptor mediates vascular effects of inhaled vehicle emissions. Am J Respir Crit Care Med. 2011; 184:82–91. [PubMed: 21493736]

Lund AK, Lucero J, Lucas S, Madden MC, McDonald JD, Seagrave JC, Knuckles TL, Campen MJ. Vehicular emissions induce vascular MMP-9 expression and activity associated with endothelin-1-mediated pathways. Arterioscler Thromb Vasc Biol. 2009; 29:511–517. [PubMed: 19150882]

Lundback M, Mills NL, Lucking A, Barath S, Donaldson K, Newby DE, Sandstrom T, Blomberg A. Experimental exposure to diesel exhaust increases arterial stiffness in man. Particle and fibre toxicology. 2009; 6:7. [PubMed: 19284640]

Mills NL, Tornqvist H, Gonzalez MC, Vink E, Robinson SD, Soderberg S, Boon NA, Donaldson K, Sandstrom T, Blomberg A, Newby DE. Ischemic and thrombotic effects of dilute diesel-exhaust inhalation in men with coronary heart disease. N Engl J Med. 2007; 357:1075–1082. [PubMed: 17855668]

Mills NL, Tornqvist H, Robinson SD, Gonzalez M, Darnley K, MacNee W, Boon NA, Donaldson K, Blomberg A, Sandstrom T, Newby DE. Diesel exhaust inhalation causes vascular dysfunction and impaired endogenous fibrinolysis. Circulation. 2005; 112:3930–3936. [PubMed: 16365212]

Mutlu GM, Green D, Bellmeyer A, Baker CM, Burgess Z, Rajamannan N, Christman JW, Foiles N, Kamp DW, Ghio AJ, Chandel NS, Dean DA, Sznajder JI, Budinger GR. Ambient particulate matter accelerates coagulation via an IL-6-dependent pathway. J Clin Invest. 2007; 117:2952–2961. [PubMed: 17885684]

Paffett ML, Zychowski KE, Sheppard L, Robertson S, Weaver JM, Lucas SN, Campen MJ. Ozone Inhalation Impairs Coronary Artery Dilation via Intracellular Oxidative Stress: Evidence for Serum-borne Factors as Drivers of Systemic Toxicity. Toxicol Sci. 2015

Pietraszek MH, Takada Y, Yan D, Urano T, Serizawa K, Takada A. Relationship between serotonergic measures in periphery and the brain of mouse. Life Sci. 1992; 51:75–82. [PubMed: 1377321]

Pope CA 3rd, Verrier RL, Lovett EG, Larson AC, Raizenne ME, Kanner RE, Schwartz J, Villegas GM, Gold DR, Dockery DW. Heart rate variability associated with particulate air pollution. Am Heart J. 1999; 138:890–899. [PubMed: 10539820]

Robertson S, Colombo ES, Lucas SN, Hall PR, Febbraio M, Paffett ML, Campen MJ. CD36 mediates endothelial dysfunction downstream of circulating factors induced by O3 exposure. Toxicol Sci. 2013; 134:304–311. [PubMed: 23650127]

Samet J, Krewski D. Health effects associated with exposure to ambient air pollution. J Toxicol Environ Health A. 2007; 70:227–242. [PubMed: 17365585]

Schisler JC, Ronnebaum SM, Madden M, Channell M, Campen M, Willis MS. Endothelial inflammatory transcriptional responses to an altered plasma exposome following inhalation of diesel emissions. Inhal Toxicol. 2015a:1–9.

Schisler JC, Ronnebaum SM, Madden M, Channell M, Campen M, Willis MS. Endothelial inflammatory transcriptional responses to an altered plasma exposome following inhalation of diesel emissions. Inhalation toxicology. 2015b; 27:272–280. [PubMed: 25942053]

Sun Q, Wang A, Jin X, Natanzon A, Duquaine D, Brook RD, Aguinaldo JG, Fayad ZA, Fuster V, Lippmann M, Chen LC, Rajagopalan S. Long-term air pollution exposure and acceleration of atherosclerosis and vascular inflammation in an animal model. JAMA. 2005; 294:3003–3010. [PubMed: 16414948]

Thomson E, Kumarathasan P, Goegan P, Aubin RA, Vincent R. Differential regulation of the lung endothelin system by urban particulate matter and ozone. Toxicol Sci. 2005; 88:103–113. [PubMed: 16081523]

Vedal S, Campen MJ, McDonald JD, Kaufman JD, Larson TV, Sampson PD, Sheppard L, Simpson CD, Szpiro AA. National Particle Component Toxicity (NPACT) Initiative Report on Cardiovascular Effects. Research report. 2013; 178:238.

Yin F, Lawal A, Ricks J, Fox JR, Larson T, Navab M, Fogelman AM, Rosenfeld ME, Araujo JA. Diesel exhaust induces systemic lipid peroxidation and development of dysfunctional pro-oxidant and pro-inflammatory high-density lipoprotein. Arterioscler Thromb Vasc Biol. 2013; 33:1153–1161. [PubMed: 23559632]

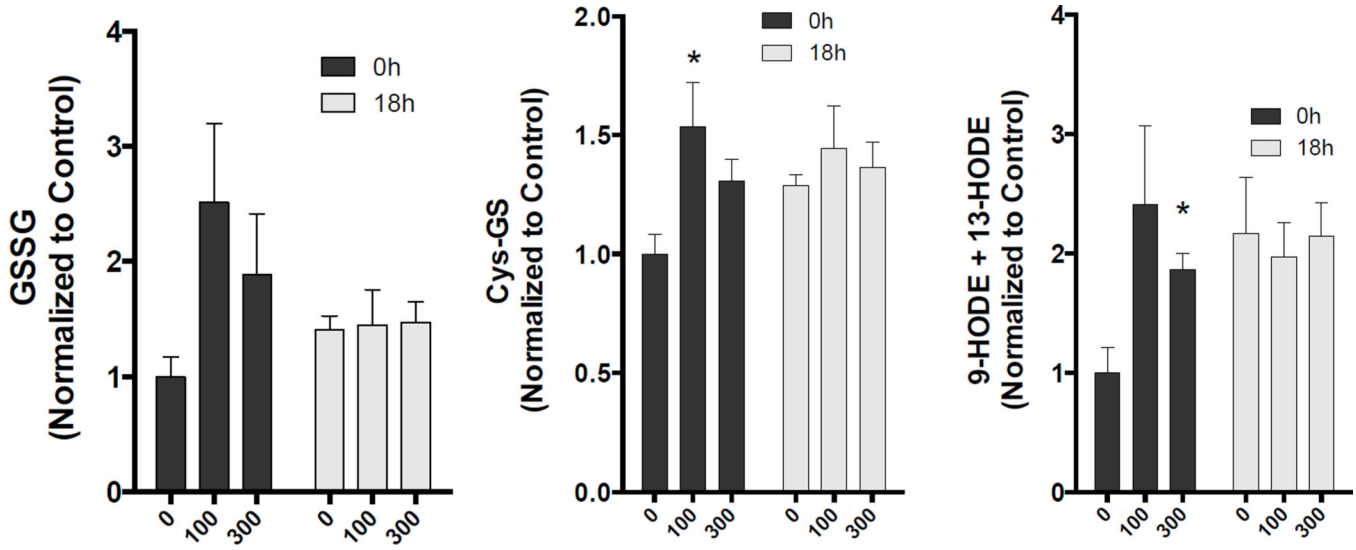

Figure 1.

Indicators of oxidative stress that were altered by MVE exposure. Asterisks denote significant difference from control ($p<0.05$).

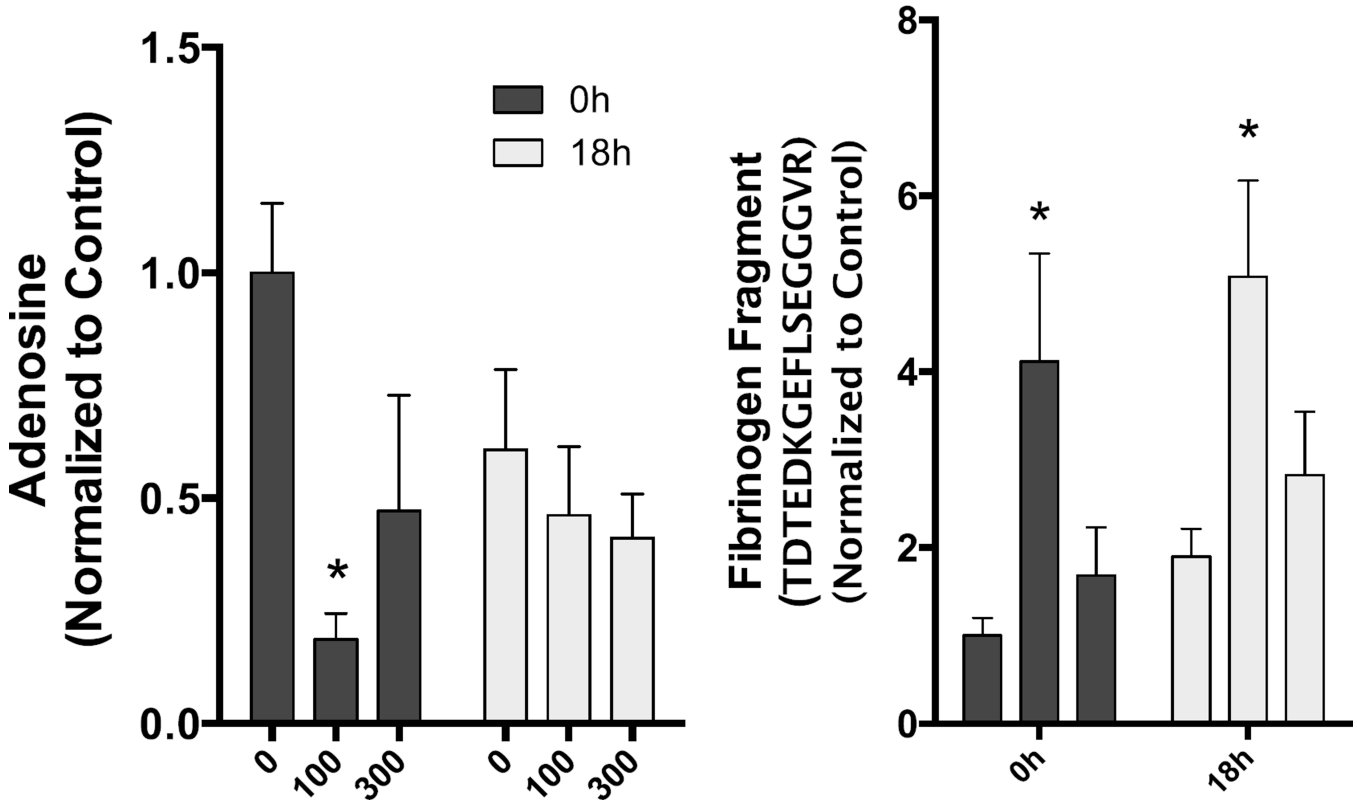

Figure 2.

Changes in adenosine and the presence of a fibrinogen fragment that were altered by MVE exposure. Asterisks denote significant difference from control ($p<0.05$).

Table 1

Exposure Atmosphere Summary (Average of 3 measurements over the 6 hour exposure).

Exposure Chamber	Particulate (μg/m^3)	NOX (ppm)	CO (ppm)
Filtered Air	3	0.049	0.60
MVE low (target 100 μg/m^3)	113	7.827	48.63
MVE high (target 300 μg/m^3)	390	7.949	50.60

Table 2

Summary of metabolomics changes in serum. Comparisons are based on change between timepoints (ie, 0h and 18h) or exposures (FA, MVE100, MVE300) at 0 h post-exposure.

Statistical Comparisons – Circadian and 0h Concentration Data						
Two-Way ANOVA Contrasts	**FA-18 / FA-0**	**MVE100-18 / MVE100-0**	**MVE300-18 / MVE300-0**	**MVE100-0 / FA-0**	**MVE300-0 / FA-0**	**MVE300-0 / MVE100-0**
Total biochemicals $p \leq 0.05$	77	107	61	114	31	14
Biochemicals (↑|↓)	65 | 12	45 | 62	32 | 29	109 | 5	30 | 1	8 | 6
Total biochemicals $0.05 < p < 0.10$	25	23	28	33	25	24
Biochemicals (↑|↓)	20 | 5	3 | 20	11 | 17	26 | 7	23 | 2	8 | 16

Table 3

Summary of metabolomics changes in serum. Comparisons are based on change between exposures (FA, MVE100, MVE300) at 18 h post exposure.

Statistical Comparisons – 18h Comparisons				
Two-Way ANOVA Contrasts	**MVE100-18 FA-18**	**MVE300-18 FA-18**	**MVE300-18 MVE100-18**	**MVE300-18 MVE100-0**
Total biochemicals $p \leq 0.05$	24	2	24	103
Biochemicals (↑|↓)	7 | 17	0 | 2	13 | 11	33 | 70
Total biochemicals $0.05 < p < 0.10$	19	6	24	38
Biochemicals (↑|↓)	6 | 13	1 | 5	15 | 9	14 | 24

Table 4

Summary of metabolomics changes in serum. Total biochemical changed based on Concentration and Time factors in the study design.

Statistical Comparisons – Total Changes			
ANOVA Main Effects	**Concentration Main Effects**	**Time Main Effects**	**Concentration:Time Interaction**
Total biochemicals $p \leq 0.05$	49	122	18
Total biochemicals $0.05 < p < 0.10$	52	31	15

Inhal Toxicol. Author manuscript; available in PMC 2017 April 01.

Table 5

Heat map of metabolites that were determined to be significantly increased by exposure to MVE. Color is relative to the degree of change relative to control (darker red = greater difference). Numbers indicate the fold-induction level. b-faced numbers are significantly increased by the ANOVA analysis, $p<0.05$.

		0h		18h	
Sub Pathway	**Biochemical Name**	**MVE100-0 FA-0**	**MVE300-0 FA-0**	**MVE100-18F A-18**	**MVE300-18 FA-18**
Glycine, Serine and Threonine Metabolism	N-acetylserine	1.17	**1.28**	1.05	0.96
	beta-hydroxypyruvate	1.12	**1.61**	1.1	0.98
Glutamate Metabolism	glutamate	**1.78**	1.14	**1.48**	1.1
	glutarylcarnitine (C5)	1.22	**1.57**	0.83	0.87
	xanthurenate	**2.84**	**1.6**	0.8	0.82
	C-glycosyltryptophan*	**1.47**	**1.21**	0.92	0.94
Leucine, Isoleucine and Valine Metabolism	2-methylbutyrylglycine	1.95	**2.42**	**1.5**	1.26
	2-hydroxy-3-methylvalerate	**1.42**	**1.82**	0.8	1.08
	3-methyl-2-oxobutyrate	1.29	**1.46**	1.11	1.14
	alpha-hydroxyisocaproate	0.8	**1.63**	0.87	0.96
Methionine, Cysteine, SAM and Taurine Metabolism	taurine	1.13	**1.92**	0.96	0.72
Creatine Metabolism	creatine	1	**1.31**	0.92	0.91
	5-methylthioadenosine (MTA)	**1.47**	**1.21**	0.98	0.88
Glutathione Metabolism Polypeptide	glutathione, oxidized (GSSG)	**2.78**	**1.9**	0.81	1.04
	cysteine-glutathione disulfide	**1.45**	**1.3**	1.01	1.06
	gamma-glutamyltryptophan	1.14	**1.25**	**1.22**	1.03
	bradykinin, des-arg(9)	**3.41**	1.38	**3.33**	1.48
Fibrinogen Cleavage Peptide	TDTEDKGEFLSEGGGVR*	3.02	1.22	**2.59**	1.49
Glycolysis, Gluconeogenesis, and Pyruvate Metabolism	lactate	1.09	**1.31**	0.91	**0.82**
	glycerate	1.08	**1.57**	**0.95**	0.78
Fructose, Mannose and Galactose Metabolism	mannose	**1.33**	**1.43**	1.09	1.15
	phosphate	1.13	**1.24**	1.13	0.94

		0h		18h	
Sub Pathway	Biochemical Name	MVE100-0 FA-0	MVE300-0 FA-0	MVE100-18F A-18	MVE300-18 FA-18
Medium Chain Fatty Acid	caproate (6:0)	**1.64**	1.18	**1.47**	1.23
	caprylate (8:0)	**1.73**	1.23	1.02	1.25
Long Chain Fatty Acid	myristate (14:0)	**2.32**	1.36	0.95	1.25
	myristoleate (14:1n5)	**2.75**	1.69	1.14	1.4
	oleate(18:1n9)	**1.82**	1.37	0.87	1.12
	linoleate(18:2n6)	**2.14**	1.3	0.78	0.96
	2-hydroxyadipate	2.29	**2.35**	1	0.96
	hexadecanedioate	1.02	1.13	**1.35**	1.14
Fatty Acid Metabolism (also BCAA Metabolism)	butyrylcarnitine	**1.63**	**1.31**	0.82	0.9
	propionylcarnitine	**1.3**	**1.3**	1.02	0.92
Fatty Acid Metabolism(Acyl Glycine)	valerylglycine	**1.82**	1.09	0.89	0.91
	valerylcarnitine	**1.82**	**1.53**	1.05	**0.61**
Carnitine Metabolism	deoxycarnitine	**1.29**	1.18	1.11	1.01
	3-hydroxydecanoate	1.27	**1.63**	1.04	1.09
	13-HODE + 9-HODE	**2.84**	1.52	0.9	0.99
Fatty Acid, Dihydroxy	12,13-DiHOME	**2.41**	**1.91**	1.03	**1**
Endocannabinoid	palmitoyl ethanolamide	**1.24**	**1.27**	1.01	1.12
Inositol Metabolism	myo-inositol	1.08	**1.36**	0.87	0.86
	1-palmitoylglycerophosphoglycerol*	0.76	1.13	**1.4**	0.91
Glycerolipid Metabolism	glycerol	**1.58**	**1.32**	1.16	1.2
	1-stearoylglycerol (1-monostearin)	1.15	1.04	**1.41**	1.14
	stearoyl sphingomyelin	0.91	**1.44**	0.84	**0.7**
	7-alpha-hydroxy-3-oxo-4-cholestenoate (7-Hc	1.04	**1.25**	1.26	0.93
Secondary Bile Acid Metabolism	deoxycholate	0.51	0.82	**4.6**	1.42
	taurodeoxycholate	1.01	0.8	**3.29**	1.19
	xanthosine	0.96	**1.42**	1.17	1.09
	uracil	1.19	**1.56**	1.25	1.04
	oxalate (ethanedioate)	**2.19**	1.55	0.98	0.92

		0h		18h	
Sub Pathway	**Biochemical Name**	**MVE100-0 FA-0**	**MVE300-0 FA-0**	**MVE100-18F A-18**	**MVE300-18 FA-18**
Chemical	2-pyrrolidinone	**1.29**	**1.22**	1	1.01
	2-ethylhexanoate	**1.45**	**1.56**	0.98	1.15

Table 6

Heat map of metabolites that were determined to be significantly decreased by exposure to MVE. Color is relative to the degree of change relative to control (darker green = greater difference). Numbers indicate the fold-induction level. b-faced numbers are significantly increased by the ANOVA analysis, $p<0.05$.

		0h		18h	
Sub Pathway	**Biochemical Name**	**MVE100-0 FA-0**	**MVE300-0 FA-0**	**MVE100-18 FA-18**	**MVE300-18 FA-18**
Glycine, Serine and Threonine Metabolism	sarcosine (N-Methylglycine)	0.85	0.81	0.76	**0.54**
Histidine Metabolism	histidine	**0.82**	1	0.99	**0.87**
	3-phenylpropionate (hydrocinnamate)	**0.54**	0.9	1.41	0.96
Tryptophan Metabolism	indoleacetate	**0.72**	1.09	1.22	0.94
	indolepropionate	**0.68**	**1.22**	1.27	1.07
	3-indoxyl sulfate	**0.72**	**0.78**	1.04	0.9
	isovalerylcarnitine	1.02	1.09	0.96	**0.81**
Urea cycle; Arginine and Proline Metabolism	arginine	**0.75**	0.95	0.89	1.01
Gamma-glutamyl Amino Acid	gamma-glutamylalanine	**0.76**	1.01	1.12	1.03
Glycolysis, Gluconeogenesis, and Pyruvate Metabolism	1,5-anhydroglucitol (1,5-AG)	1.12	1.12	**0.78**	**0.84**
	ribose	0.92	1.12	**0.52**	0.95
	fumarate	**0.63**	0.99	1.29	1.03
	malate	**0.65**	1.08	1.06	0.98
Leucine, Isoleucine and Valine Metabolism	eicosapentaenoate (EPA; 20:5n3)	0.98	0.92	**0.61**	1.12
	dihomo-linolenate (20:3n3 or n6)	1.58	1.14	**0.59**	0.99
	azelate (nonanedioate)	**0.63**	0.89	0.87	0.8
	valerylcarnitine	**1.82**	**1.53**	1.05	**0.61**
	scyllo-inositol	0.95	1.3	**0.56**	**0.73**
	1-lignoceroylglycerophosphocholine (24:0)*	1.62	0.31	**0.11**	**0.07**
	1-linoleoylglycerophosphoethanolamine*	1	0.94	**0.54**	0.77
	1-arachidonoylglycerophosphoethanolamine*	1.13	1.05	**0.51**	0.88
	2-arachidonoylglycerophosphoethanolamine*	1.21	0.99	**0.61**	0.81

		0h		18h	
Sub Pathway	**Biochemical Name**	**MVE100-0 FA-0**	**MVE300-0 FA-0**	**MVE100-18 FA-18**	**MVE300-18 FA-18**
	1-eicosatrienoylglycerophosphoethanolamine	1	1.18	**0.51**	0.89
	1-docosahexaenoylglycerophosphoethanolan	1.14	1.04	**0.58**	0.82
	1-linoleoylglycerol (1-monolinolein)	1.38	1.35	**0.45**	0.82
	2-linoleoylglycerol (2-monolinolein)	1.18	1.74	**0.49**	0.74
	1-arachidonylglycerol	1.42	1.25	**0.59**	0.98
Purine Metabolism, (Hypo)Xanthine/Inosine containing	inosine	0.94	0.97	**0.56**	0.8
	xanthine	2.07	1.45	**0.44**	0.9
	adenosine	**0.14**	**0.66**	0.86	0.68
	guanosine	0.69	0.64	**0.49**	0.78
Benzoate Metabolism	hippurate	**0.73**	1.1	0.96	0.95
	4-hydroxyhippurate	1.17	0.99	**0.75**	**0.72**
	4-methylcatechol sulfate	**0.73**	0.87	**1**	0.85
	4-vinylphenol sulfate	**0.5**	0.84	0.9	0.76
Food Component/Plant	cinnamoylglycine	**0.79**	0.99	1.1	1.23
	stachydrine	0.99	1.06	**0.77**	**0.75**